Transport and fate of bacteria in porous media: Coupled effects of chemical conditions and pore space geometry

Saeed Torkzaban,[1] Shiva S. Tazehkand,[2] Sharon L. Walker,[1] and Scott A. Bradford[3]

[1] Experimental and theoretical studies were undertaken to explore the coupled effects of chemical conditions and pore space geometry on bacteria transport in porous media. The retention of *Escherichia coli* D21g was investigated in a series of batch and column experiments with solutions of different ionic strength (IS) and ultrapure quartz sand. Derjaguin–Landau–Verwey–Overbeek (DLVO) calculations and results from batch experiments suggested that bacteria attachment to the sand surface was negligible when the IS was less than or equal to 50 mM. Breakthrough data from column experiments showed significant cell retention and was strongly dependent on the IS. This finding indicates that cell retention was dependent on the depth of the secondary energy minimum which increases with IS. When the IS of the influent bacteria-free solution was decreased to 1 mM, only a small fraction of the retained bacteria was released from the column. The remaining retained bacteria, however, were recovered from the sand, which was excavated from the column and suspended in a cell-free electrolyte having the original IS. These observations suggest that the solution chemistry is not the only parameter controlling bacteria retention in the porous media. Computational simulations of flow around several collector grains revealed the retention mechanism, which is dependent on both the solution chemistry and the pore space geometry. Simulations demonstrate that the pore space geometry creates hydrodynamically disconnected regions. The number of bacterial cells that may be transported to these relatively "immobile" regions will theoretically be dependent on the depth of the secondary energy minimum (i.e., the IS). Once bacteria are trapped in these immobile regions, reduction of the secondary energy minimum does not necessarily release the cells owing to hydrodynamic constraints.

1. Introduction

[2] An improved understanding of the mechanisms that govern the fate and transport of microbes in the subsurface is needed for a variety of remediation and water quality purposes [*Ginn et al.*, 2002]. For example, predicting the fate and transport of pathogenic bacteria in groundwater requires knowledge on the processes controlling cell deposition in porous media. Bioremediation and/or bioaugmentation strategies to clean up recalcitrant chemicals in subsurface environments could also be greatly improved by efficient delivery of specialized bacteria to targeted locations in the subsurface.

[3] Considerable research has been devoted to understand the effects of the physical, chemical, and biological factors that control the transport and fate of bacteria in aquatic systems (e.g., see the review articles of *Murphy and Ginn* [2000], *Harvey and Harms* [2001], *Foppen and Schijven* [2006]). The factors investigated include solution chemistry [*Gannon et al.*, 1991; *Martin et al.*, 1991; *Jewett et al.*, 1995], cell type [*van Loosdrecht et al.*, 1987a; *Gannon et al.*, 1991], hydrophobic interactions [*van Loosdrecht et al.*, 1987b; *Schafer et al.*, 1998], motility [*Camesano and Logan*, 1998; *Vigeant et al.*, 2002] surface charge characteristics [*Gross et al.*, 2001], and surface features (e.g., lipopolysaccharides, fimbriae) [*Herald and Zottola*, 1989; *Walker et al.*, 2004]. Despite these attempts, the mechanisms and interconnected nature of these parameters governing the retention of bacterial cells in porous media are still not fully known.

[4] Traditionally, the attachment of bacteria to solid surfaces has been generally treated similar to that of inorganic colloidal particles [*Rijnaarts et al.*, 1995; *Redman et al.*, 2004]. In these cases, DLVO theory [*Derjaguin and Landau*, 1941; *Verwey and Overbeek*, 1948] has been applied to explain the attachment behavior [*Rijnaarts et al.*, 1995; *Simoni et al.*, 2000; *Poortinga et al.*, 2002]. Specifically, DLVO theory states that the interactions between a colloid and a collector surface can be expressed as the sum of the attractive van der Waals and electrostatic double layer interactions, which can be either attractive or repulsive. Since both the bacteria and collector surfaces are negatively charged in many natural environments, DLVO

[1] Department of Chemical and Environmental Engineering, University of California, Riverside, California, USA.
[2] Department of Earth Sciences, Utrecht University, Utrecht, Netherlands.
[3] U.S. Salinity Laboratory, Agricultural Research Service, U.S. Department of Agriculture, Riverside, California, USA.

calculations indicate the presence of a repulsive force between the bacteria and solid surfaces. Despite these predictions, it has been observed that bacteria are often retained in porous media [*Redman et al.*, 2004; *Walker et al.*, 2004; *Smets et al.*, 1999]. There have been some attempts to resolve discrepancies between DLVO predictions and observed retention data by considering non-DLVO forces (e.g., Lewis acid-base interactions) into the so-called extended DLVO calculations [*Simoni et al.*, 2000; *Meinders et al.*, 1995; *Azeredo et al.*, 1999]. In some cases, these observed discrepancies were attributed to the existence of local surface charge heterogeneities on the sand grains, which are not accounted for by classical DLVO theory [*Truesdail et al.*, 1998].

[5] A growing body of evidence suggests that the secondary energy minimum can play a significant role to the retention of colloidal particles in saturated porous media [*Franchi and O'Melia*, 2003; *Hahn et al.*, 2004; *Tufenkji and Elimelech*, 2004, 2005]. For example, *Redman et al.* [2004] systematically examined the adhesion of an *Escherichia coli* bacterial strain to quartz sand in the presence of repulsive interactions. Bacterial attachment increased with the solution ionic strength (IS), despite DLVO calculations which indicated a sizable energy barrier to attachment, and therefore it was concluded that bacteria deposition occurred in the secondary energy minimum. However, when *Redman et al.* [2004] exposed the deposited bacteria to a very low-solution IS, only a portion of the deposited cells in the column was recovered in the effluent. The authors were not able to provide a full explanation for the partial release of the bacteria. The transport and retention behavior of inorganic colloids have also been observed to be highly dependent on solution chemistry under unfavorable conditions [*Tufenkji and Elimelech*, 2004, 2005; *Bradford et al.*, 2007]. Similarly, these studies have shown that once colloids are retained in the column at a given solution IS, reducing the IS does not necessarily release all of the colloids. It is therefore possible that there are other mechanisms, beside physicochemical forces, involved in bacterial and colloidal retention in porous media.

[6] Mass transfer of colloids to collector surfaces occurs via diffusion, interception, and sedimentation [*Yao et al.*, 1971]. Attachment involves collision with and subsequent retention of colloids on the grain surface. Therefore, once a colloid approaches the collector surface, attachment depends on the summation of forces and torques that act on the particle at this location [*Cushing and Lawler*, 1998; *Bergendahl and Grasso*, 2000; *Torkzaban et al.*, 2007]. The forces acting on a particle in the vicinity of the collector surface include physicochemical forces as incorporated by DLVO theory, hydrodynamic (drag and lift), gravity, buoyancy, and Brownian forces [*Cushing and Lawler*, 1998]. Among these forces the DLVO and hydrodynamic drag forces have been found to be dominant under laminar flow conditions [*Torkzaban et al.*, 2007]. Under chemically favorable attachment conditions (resulting in attachment in the primary minimum of the DLVO profile), it is reasonable to assume that hydrodynamic forces will have a negligible effect on particle attachment owing to the very large adhesive force between the bacteria and the collector. However, under chemically unfavorable conditions the hydrodynamic drag force acting on the colloids adjacent to the collector surface may have a substantial influence on the attachment efficiency of colloids to porous media [*Torkzaban et al.*, 2007; *Bradford et al.*, 2007]. The relative impact of hydrodynamic forces on bacteria deposition in porous media has received considerably less attention as physicochemical forces in recent literature.

[7] In this study, the transport and retention behavior of a well-characterized *Escherichia coli* strain (D21g) in solutions with various IS were systematically investigated. Emphasis was placed on the coupled role of pore space geometry and system hydrodynamics on bacteria retention, and on whether the observed deposition behavior can be explained by combination of classical DLVO theory and system hydrodynamics. To minimize charge heterogeneity effects, highly cleaned, ultrapure quartz sand was selected as the porous medium. Following recovery of cell breakthrough data in the column experiments, the IS of the influent cell-free solution was decreased to 1 mM and the column was flushed for several more pore volumes. Mass balance calculations for the bacteria were conducted from the breakthrough curve information and the final retained cells in the column. A series of batch experiments were also carried out to better determine cell attachment in the absence of pore structure. Additionally, computational simulations considering the influence of hydrodynamic conditions and DLVO forces on bacteria retention to several sand grains were conducted. Analysis of the simulation results suggests that the pore space geometry and the depth of the secondary energy minimum both play an important role in bacteria retention under unfavorable attachment conditions and explain experimental observations.

2. Material and Methods

2.1. Bacteria, Sand, and Electrolyte Solutions

[8] *Escherichia coli* D21g, which is a Gram-negative, non motile bacterial strain with negligible amounts of extracellular polysaccharide (EPS) on its surface, was chosen for the experiments [*Walker et al.*, 2004]. Cells were grown in 200 ml Luria-Bertani broth (LB broth, Fisher Scientific, Fair Lawn, NJ) supplemented with 0.03 mg/l of gentamicin (Sigma, St. Louis, MO) at 37 °C for 3 hours until reaching midexponential phase, at which time they were harvested for use in experiments. The bacterial suspension was centrifuged to separate whole cells from the growth medium. The supernatant was decanted and the pellet was resuspended in a 10 mM KCl solution. To ensure all traces of growth medium were removed, the process of centrifuging, decanting, and resuspending in the electrolyte solution was repeated three times. More details about the cell preparation and handling protocols are given in the work of *Walker et al.* [2004].

[9] Ultrapure quartz sand (Iota® quartz, Unimin Corp., NC) was employed as the porous media for column experiments. The sand medium grain size (d_{50}) was 205 μm with a coefficient of uniformity (d_{60}/d_{10}) equal to 1.26. Prior to use, the sand was treated with 12 N HCl (Fisher Scientific) for at least 24 h to remove any impurities, rinsed thoroughly with deionized water, baked at 800 °C for 8 h, and then boiled in deionized water for 1 h to rehydrate the sand surfaces.

[10] Five different electrolyte solutions were prepared by addition of reagent-grade KCl (Fisher Scientific) to

Table 1. Electrokinetic Properties of Bacteria and Quartz Sand As Well As the Calculated Depth of the Secondary Energy Minimum (Φ_{min2}), the Repulsive Energy Barrier (Φ_{max}), and the Distance of the Secondary Minimum From the Surface (h)

Ionic Strength, mM	Zeta Potential, mV		Φ_{min2}, $k_b T_k$	Φ_{max}, $k_b T_k$	h, nm
	Quartz Grains[a]	Bacteria			
1	−38	−61	−0.09	2250	120
10	−22	−49	−1.27	262	32
30	−13.6	−38	−4.4	86	14.5
50	−12	−32	−7.5	44	10
100	−11.2	−21	NB[b]	0	NB[b]

[a]Values estimated from data reported in the work of *Redman et al.* [2004].
[b]NB, no energy barrier to deposition in the primary minimum.

deionized water to achieve IS of 1, 10, 30, 50, and 100 mM. The solution pH was unadjusted (5.6 to 5.8). For the experiments discussed below, bacteria suspensions containing between 10^7 and 10^8 cells/ml were prepared using these various electrolyte solutions.

2.2. Electrokinetic Characterization and DLVO Calculations

[11] The zeta potential of bacterial cells was measured using a ZetaPals instrument (Brookhaven Instruments Cooperation, Holtsville, NY). The measurements were repeated five times for each cell suspension and the average values are reported in Table 1. The zeta potential of the quartz sand utilized in calculations was presented in the work of *Redman et al.* [2004].

[12] DLVO theory was used to calculate the total interaction energy (sum of London-van der Waals attraction and electrostatic double-layer repulsion) for bacteria upon close approach to quartz surfaces (assuming sphere-plate interactions) for the various solution chemistries (IS = 1, 10, 30, 50, and 100 mM). Retarded London-van der Waals attractive interaction force was determined from the expression of *Gregory* [1981] utilizing a value of 6.5×10^{-21} J for the Hamaker constant [*Simoni et al.*, 2000] to represent the bacteria-water-quartz system. In these calculations, constant-potential electrostatic double layer interactions were quantified using the expression of *Hogg et al.* [1966], with zeta potentials (Table 1) in place of surface potentials.

2.3. Batch Experiments

[13] Batch experiments were carried out to determine the extent of bacterial attachment to quartz sand in the absence of pore structure (entire system in motion). These experiments were conducted by placing 10 g of sand and 10 ml of a known initial concentration of bacterial suspension into 15 ml centrifuge tubes with the temperature kept at approximately 20°C. Four different solution ionic strengths were considered in the batch studies (10, 30, 50, 100 mM). The suspension and sand were allowed to equilibrate for 1 h by gently rotating the tubes end over end (15 rpm) on a tube rotator (Fisher Scientific). The initial and final concentrations of bacteria in the suspension were determined using a UV/vis spectrophotometer (SP-890, Barnstead International, Dubuque, IA) at 240 nm after setting the tube to rest for a few minutes. All experiments were performed in duplicate. A control experiment of sand and electrolyte

solution without bacteria was also performed to measure the background colloid concentration originating from the sand. The background colloid concentration was lower than the bacterial concentration by more than two orders of magnitude, and was consistent in different batch experiments with the same IS.

[14] The concentration of the attached bacteria to the sand grains in each tube was determined using the following equation:

$$S_{eq} = \frac{(C_I - C_f) \times V}{M_s} \tag{1}$$

where M_s is the total mass of sand in the tube (M, where M denotes units of mass), V is the volume of suspension added to the tube (L^3; where L denotes units of length), and C_I is the initial concentration of the bacteria in the liquid phase ($N_c L^{-3}$; where N_c denotes number of cells), C_f is the final concentration of the bacteria in the liquid phase ($N_c L^{-3}$), and S is concentration of bacteria on the solid phase ($N_c M^{-1}$).

2.4. Column Experiments

[15] Column experiments were conducted using 10 cm glass-chromatography column with 1 cm inner diameter (Omnifit, Boonton, NJ). The sand was wet-packed in the column following the procedure detailed in the work of *Bradford et al.* [2002] to produce a homogeneous packing. Prior to bacteria transport experiments, a solution containing 0.2 mM $NaNO_3$ (Fisher Scientific) was applied to the column using a syringe pump (KD Scientific Inc., New Hope, PA) to determine the dispersion coefficient and the porosity of the porous media. Porosity was also determined gravimetrically. Both approaches gave similar values of porosity of about 0.43. The tracer breakthrough curve was obtained by measuring the absorbance of the effluent at 204 nm by using a spectrophotometer. The column was flushed with about five pore volumes of the electrolyte solution to equilibrate the IS of the system.

[16] A bacteria suspension was introduced into the column using a syringe pump to provide an approach (superficial) velocity of 0.66 cm/min. The bacteria suspension was applied for four pore volumes (approximately 24 min), followed by bacteria-free solution of the same IS for several more pore volumes. An additional pulse of a bacteria-free solution with a low IS (1 mM KCl) was then applied to the column for several more pore volumes. The introduction of this low-solution IS was continued until the cell concentration had decayed to background absorbance levels.

[17] Following the bacteria transport experiments, the total number of retained bacteria in the sand column was determined by placing the sand in a vial containing excess amounts of an electrolyte solution of the original IS that was used in the transport experiment. The vial was slowly shaken for several minutes to liberate any reversibly retained bacteria (in the absence of a constant pore structure). The concentration of the bacteria in the excess solution was measured spectroscopically and the volume of solution and mass of dry sand was determined.

[18] The HYDRUS-1D code [*Simunek et al.*, 2005] was used to simulate the bacteria transport through the columns. Relevant aspects of this code are described below. The code numerically solves the Fickian-based advection-dispersion
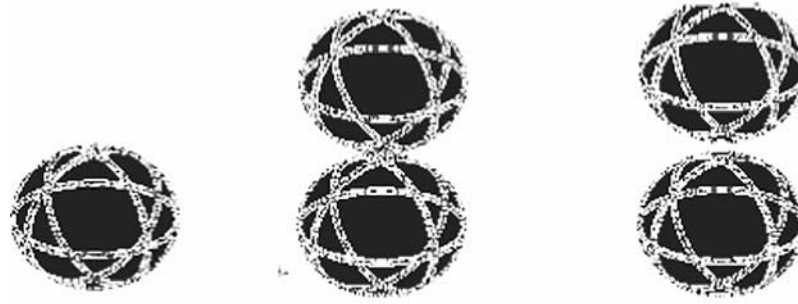
Figure 1. Schematic representation of porous media with three different models; namely, a single sphere, two spheres in contact, and two spheres not in contact. The spheres in each model are placed in a cell in order to account for porosity (in analogy to filtration theory). The spheres radii in all three models are 100 μm, and the distance between the two spheres in the TSIC and TSNIC models is 0 and 30 μm, respectively.

equation that accounts for bacteria deposition in the column:

$$\frac{\partial C}{\partial t} = \lambda v \frac{\partial^2 C}{\partial z^2} - v \frac{\partial C}{\partial z} - r_d \qquad (2)$$

where C is the concentration of bacteria in the liquid phase ($N_c L^{-3}$), λ is the dispersivity (L), v is the average pore water velocity (LT^{-1}; where T denotes units of time), and r_d is the mass transfer rate of bacteria in the aqueous phase to the solid phase ($N_c L^{-3} T^{-1}$). The value of r_d is given by:

$$\rho_b \frac{\partial S}{\partial t} = r_d = n K_{dep} \left(1 - \frac{S}{S_{max}} \right) C \qquad (3)$$

where ρ_b is the soil bulk density (ML^{-3}), n is the porosity (−), K_{dep} is the bacterial deposition coefficient (T^{-1}), and S_{max} is the maximum concentration of deposited bacteria on the sand ($N_c M^{-1}$). HYDRUS 1D is coupled to a nonlinear least squares optimization routine based upon the Levenberg-Marquardt algorithm [*Marquardt*, 1963] to fit model parameters to breakthrough curves.

2.5. Fluid Flow Around Collectors and Cell Retention

[19] Packed beds of granular media have often been represented by the single sphere-in-cell (SS) model [*Happel*, 1958; *Payatakes et al.*, 1974]. However, in this model the effect of neighboring collectors on the fluid flow and colloid retention to the collector is neglected. Here, we propose two additional simple models for representing the porous media, namely, two spheres in contact (TSIC) and two spheres not in contact (TSNIC). The spheres in these two models are placed in a cell, as for the single sphere-in-cell model. The diameter of the spheres in all three models is 200 μm and in the case of TSIC and TSNIC models, the center line of the spheres is parallel to the direction of the fluid flow. The distance between the two spheres is zero in the TSIC model and 30 μm apart in the TSNIC model as illustrated in Figure 1. These two sphere−based models are proposed to capture more features of real porous media such as small pore spaces formed at grain-to-grain contacts and the influence of neighboring grains than the single sphere model.

[20] To compute the hydrodynamic forces acting on a bacterium near the collector surface, the fluid velocity field around the collector must be known. When the Reynolds number of the flow is sufficiently small, the inertia terms in the Navier-Stokes equations can be neglected [*Bird et al.*, 2002]. It follows that the equations governing the motion of fluid flow around single or two spherical collectors is described by Stokes and continuity equations as:

$$\nabla p = \mu \nabla^2 v, \qquad \nabla \bullet v = 0 \qquad (4)$$

where p is the water pressure ($ML^{-1}T^{-2}$), v is water velocity (LT^{-1}), and μ is the fluid viscosity ($ML^{-1}T^{-1}$). The exact solution for the Stokes flow past spherical bodies in unbounded conditions (infinite cell size) has been previously obtained by *Stimson and Jeffery* [1926], and *Cooley and O'Neill* [1969] analytically solved Stokes equation for two spheres not in contact and in contact, respectively. In the case of spheres bounded in a cell that were considered in this work, the above equations were solved numerically in an axisymmetrical coordinate system using the COMSOL software package (COMSOL, Inc., Palo Alto, CA) to determine the fluid velocity field around the collector(s). The computational mesh was refined to submicron-sized elements near the collector surface to yield the fluid velocity at the center of the bacteria in the vicinity of the collector. A no-slip boundary condition was imposed along the collector surface and a perfect slip boundary condition was set at the side boundaries of the cell surrounding the collectors. To reflect typical column experiment conditions, the simulations were performed with an average water velocity of 0.66 cm/min which is equal to the average approach velocity in the column experiment. Finally, a fixed pressure difference between the inlet and outlet boundary of the cell was applied for each model (SS, TSIC, and TSNIC) in order to achieve the desired approach velocity.

[21] Once bacteria cells are transported to the collector surface, bacteria retention will depend on a balance of forces and torques that act on bacteria at this location [*Cushing and Lawler*, 1998; *Bergendahl and Grasso*, 2000; *Torkzaban et al.*, 2007]. A detailed description for examining the coupled effects of hydrodynamic and physicochemical conditions on colloid attachment to a collector has recently been described by *Torkzaban et al.* [2007]. Only an abbreviated description is given below. It should be

mentioned that the bacteria were assumed to be spherical in shape for the sake of simplicity in this analysis.

[22] Interaction energies between bacteria and the solid surface are typically calculated using DLVO theory. The corresponding resisting (adhesive) torque ($T_{resisting}$; ML^2T^{-2}) for cells attached in either the secondary or primary minimum of the DLVO interaction energy profile is represented by the net adhesive force (F_A, MLT^{-2}) acting on a lever arm (l_x, L) as:

$$T_{resisting} = F_A l_x \qquad (5)$$

The value of the F_A in equation (5) is estimated as Φ_{min}/h [*Israelachvili*, 1992]; where Φ_{min} (ML^2T^{-2}) is the absolute value of the secondary or primary minimum interaction energy and h is the separation distance between the bacterium and the collector surface. The value of l_x is estimated using JKR theory [*Johnson et al.*, 1971; *Israelachvili*, 1992; *Soltani and Ahmadi*, 1994; *Bergendahl and Grasso*, 2000; *Torkzaban et al.*, 2007; *Ahmadi et al.*, 2007] by assuming no direct physical contact between the bacteria and the collector surface.

[23] Hydrodynamic forces will also act on cells that are in the vicinity of the solid-water interface as a result of water flow. When the water flow is laminar, the lift force acting on the cells perpendicular to the interface is negligible [*Soltani and Ahmadi*, 1994]. The drag force that act on the bacteria tangential to the interface, however, is significant and can be calculated using an equation developed by *Goldman et al.* [1967] and *O'Neill* [1968]. The corresponding driving torque ($T_{driving}$; ML^2T^{-2}) acting on cells in the vicinity of the solid interface owing to the hydrodynamic shear force is given as [*Goldman et al.*, 1967; *O'Neill*, 1968; *Sharma et al.*, 1992]:

$$T_{driving} = 1.4 r_c F_D \qquad (6)$$

where F_D (MLT^{-2}) is the drag force that act on the bacterium in the vicinity of the collector surface and r_c is the equivalent radius of the bacterium.

[24] Lifting, sliding, and rolling are the hydrodynamic mechanisms that can cause bacteria removal from an interface [*Soltani and Ahmadi*, 1994; *Bergendahl and Grasso*, 2000; *Ahmadi et al.*, 2007]. Rolling has been reported to be the dominant mechanism of hydrodynamic detachment from solid surfaces under laminar flow conditions [*Tsai et al.*, 1991; *Bergendahl and Grasso*, 1998, 1999]. Rolling occurs when $T_{resisting}$ is overcome by $T_{driving}$ from hydrodynamic forces [*Johnson*, 1985].

3. Results and Discussion

3.1. DLVO Calculations

[25] Table 1 shows that the zeta potential of the bacteria and sand becomes less negative as the IS increased owing to compression of the thickness of the electrostatic double layer [e.g., *Elimelech et al.*, 1998]. This data was used in DLVO theory calculations to estimate the total interaction energy between bacteria and the quartz collectors under the various solution chemistries (IS = 1, 10, 30, 50, and 100 mM). At an IS of 100 mM, the DLVO calculations predict no energy barrier exists to bacteria deposition on the

Table 2. Fitted Model Parameters Obtained Using Hydrus-1D for Various Solution Ionic Strengths[a]

Ionic Strength, mM	K_{dep}, min^{-1}	S^*_{max}, g^{-1}	M_{tran}, %	M_{elu} %	M_{sand} %	M_{total} %
10[b]	0.041 ± 0.01	0.4 ± 0.07	75	6.6	23	105
10	0.06 ± 0.01	0.35 ± 0.08	76.5	4.2	27	108
30[b]	0.121 ± 0.07	1.7 ± 0.06	50	13.8	40	104
30	0.09 ± 0.05	1.4 ± 0.05	61	11.2	35	107
50[b]	0.29 ± 0.02	3.9 ± 0.7	22	26.7	55.6	104
50	0.25 ± 0.06	4.1 ± 0.3	26.5	28.6	55	110
100[b]	0.90 ± 0.13	-	<2	58.4	17.4	78
100	0.91 ± 0.2	-	<2	60.4	20	81

[a]Also shown are the percentages of bacteria recovered during the bacteria transport (M_{tran}), during elution with the low-solution ionic strength (M_{elu}), from the sand (M_{sand}), and the total mass (M_{total}). The parameter $S^*_{max} = S_{max}/N_{ic}$; where N_{ic} is the number of colloids in a unit volume of influent suspension.
[b]Results are shown in Figure 2.

collector. In this case, bacteria cells may be strongly attached to the quartz sand in the primary energy minimum. At ionic strengths equal or less than 50 mM, the DLVO calculations predict the presence of substantial repulsive energy barriers (ranging from 44 $k_b T_k$ at 50 mM to over 2250 $k_b T_k$ at 1 mM, where k_b is the Boltzmann constant and T_k is the absolute temperature) to bacteria interaction with the sand surface in the primary energy minimum. The bacteria may still interact with the sand surface, however, by retention in a secondary energy minimum for which the depth increases in magnitude with IS. Table 1 provides the calculated values for depth and separation distance between the bacteria and quartz for the secondary minimum at each IS.

3.2. Attachment in the Absence of Pore Structure

[26] The distribution coefficient (K_D; L^3M^{-1}) was determined from the measured linear adsorption isotherm to quantitatively compare the effect of solution IS on the bacteria attachment where the pore structure did not exist (batch experiments). The value of K_D was determined from equation (1) as C_f/S_{eq}. The value of K_D was practically zero for all the experiments conducted at the solution IS of 10, 30, and 50 mM. This finding is consistent with the unfavorable conditions for attachment predicted by DLVO calculations, and also confirms the absence of chemical heterogeneities such as positively charged metal oxides on the sand surface. The K_D value for the experiment in IS of 100 mM, however, was 12 cm^3 g^{-1} of sand and therefore substantial attachment of cells occurred to the sand. This observation also shows qualitative agreement with DLVO calculations that predicted no energy barrier to attachment when the IS was 100 mM.

3.3. Column Experiments

[27] Bacteria transport experiments were duplicated at each IS. Summary information for these experiments is given in Table 2. Representative observed and simulated bacteria breakthrough curves for the various solution ionic strengths are presented in Figure 2. Here the normalized effluent concentration (C/C_0) is plotted against the number of pore volumes. The deposition of bacteria increased with the IS of the electrolyte solution. Notably, more than 98% of
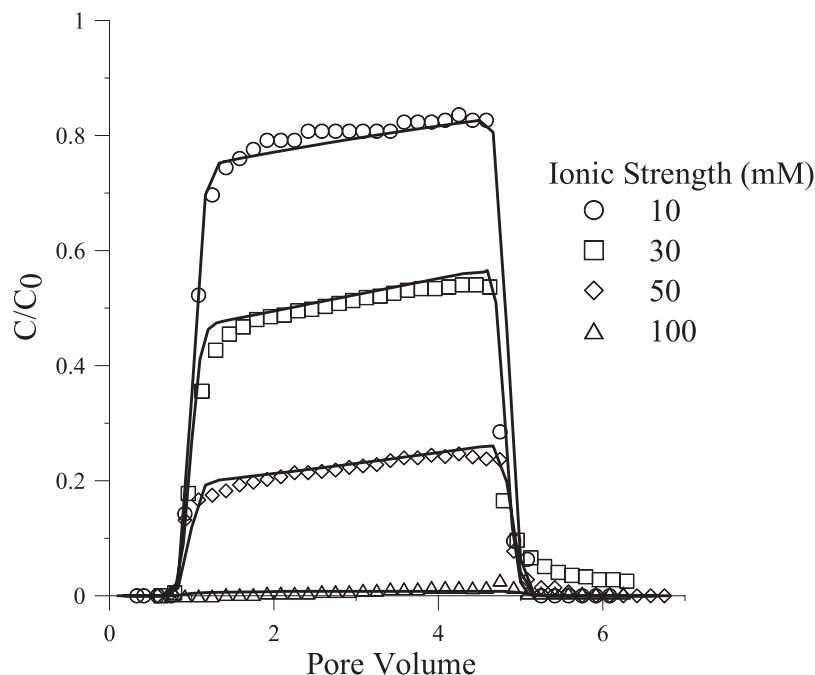
Figure 2. Observed (symbols) and simulated (lines) breakthrough concentrations of bacteria for different solution ionic strengths.

the input bacteria were retained in the column at the highest IS (100 mM). When the IS was less than or equal to 50 mM, the effluent concentration increased slowly with time toward a steady state level. Potential mechanisms causing this behavior include: bacteria detachment from the sand and blocking or filling of available locations for bacteria deposition. Blocking or filling of available locations for deposition seems to be a more likely explanation, because detachment produced insignificant tailing in the breakthrough curves.

[28] To quantitatively investigate the effect of IS on bacteria transport, the deposition rate coefficient (K_{dep}) and maximum concentration of deposited cells (S_{max}) were determined for each experiment by fitting the breakthrough data to the solution of equations (2) and (3). It should be mentioned that the dispersivity (λ) required in these simulations was estimated by fitting the solution of equation (2) to the tracer (NaNO$_3$) breakthrough data (data not shown). This value of λ was low (0.04 cm) as expected for a 10 cm column. For the bacteria transport experiments, the agreement between modeled and measured concentrations is generally good with the coefficient of linear regression (R^2) values ranging from 0.94 to 0.99. The value of K_{dep} and S_{max} increased with solution IS (Table 2). It is worth noting that because the slope of the rising limb of the breakthrough curve in the 100 mM experiment was negligible, a unique value for S_{max} was not possible. The mass fraction of bacteria that was recovered in the effluent during the bacteria transport stage (M_{tran}) was also determined and decreased with increasing IS.

[29] At first glance, it is tempting to attribute the increasing trend of bacteria deposition in the column with IS solely to chemistry induced attachment. However, this is not consistent with the observed negligible bacteria attachment that occurred in the batch experiments (except at 100 mM). If chemical interaction alone controlled retention of cells within the porous media, then batch tests should more closely follow the trend obtained in the column experiments. However, this was not the case. To better determine the role of solution IS on bacteria deposition, additional information was collected in the column experiments. Specifically, following recovery of the bacteria breakthrough data each column was flushed with several additional pore volumes of 1 mM solution before excavating the sand to determine the deposited cell mass.

[30] Figure 3 presents the recovered bacterial concentrations in the effluent as a function of pore volumes after flushing the column with 1mM solution. The corresponding bacteria breakthrough curves for the various solution ionic strengths were presented in Figure 2. The observed cell peak upon change of solution IS has typically been ascribed to release of colloids that were associated with the solid surface via the secondary minima [*Franchi and O'Melia*, 2003; *Hahn and O'Melia*, 2004] and the primary minima [*Ryan and Elimelech*, 1996]. In fact, the release of previously deposited colloidal particles by lowering the solution IS has been used as supportive evidence for particle deposition in the secondary energy minimum [*Redman et al.*, 2004; *Tufenkji and Elimelech*, 2005]. Table 2 presents the mass fraction of introduced bacteria that were recovered during elution with the low-solution IS (M_{elu}). Notice that just a fraction of the input bacteria were recovered in the effluent when the 1 mM solution was flushed through the columns. M_{elu} data ranges from about 5% when the bacteria were deposited with 10 mM solution to 60% when the cells were deposited with 100 mM solution. In other words, in the experiments conducted using 10 and 100 mM solutions, 85 and 40% of the retained cells, respectively, were not released when the IS of the eluting solution was lowered to 1 mM. It is worthwhile to mention that when the initial bacteria transport experiment was conducted in a solution with IS of 1 mM, approximately 99% of the introduced bacteria was recovered in the effluent (data not shown).
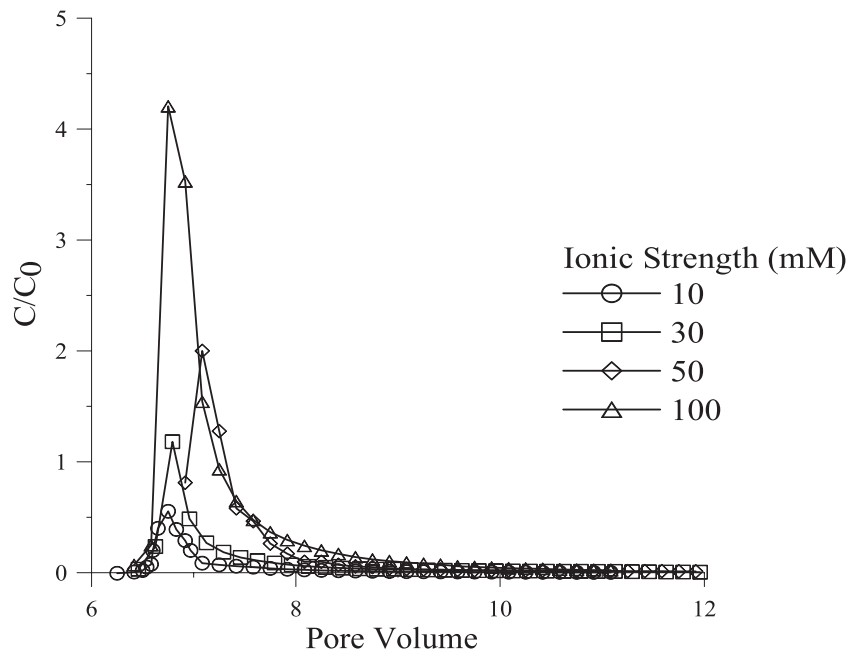
Figure 3. Observed effluent concentrations of bacteria obtained from the column when the influent was switched to the low-solution IS of 1mM. In these experiments the bacteria transport experiments were conducted with different solution ionic strengths (the main breakthrough curves are presented in Figure 2).

[31] The remaining bacteria in the column after elution with the low-solution IS were recovered when the pore structure was eliminated by excavation and suspending the sand in electrolyte solution (same IS as utilized in the original transport experiments). Table 2 also shows the mass fraction of cells that were recovered from the sand (M_{sand}), as well as the total mass (M_{total}) for the column experiments. When the IS was less than or equal to 50 mM, the total mass balance was very good (between 104 to 108%). This finding indicates that the bacteria were not irreversibly attached to the quartz grain in the primary energy minimum. For the experiments conducted in 100 mM solution, the value of M_{total} was somewhat lower (approximately 80%). In this case, slight mass balance errors likely occurred owing to attachment of cells in the primary minimum when the excavated sand was placed in 100 mM solution. Both batch experiments and DLVO calculations support this hypothesis.

[32] All of the above observations strongly indicate that the solution chemistry plays an important role in bacteria deposition in the porous media. Many other researchers have reported a similar dependence of colloid transport on IS under unfavorable attachment conditions [e.g., *Li et al.*, 2004; *Tufenkji and Elimelech*, 2004, 2005; *Bradford et al.*, 2007]. However, the batch experiments and the low IS elution results discussed above also provide further evidence that solution chemistry-induced attachment is not the sole mechanism controlling the deposition. In particular, recovering the remaining deposited bacteria by suspending the sand in a solution indicates that the pore structure may play an important role in the bacteria retention process.

3.4. Analysis of Resisting and Driving Torques

[33] To further explore the underlying mechanisms that control bacteria retention, an analysis of the resisting (from

adhesive force) and driving (from drag force) torques on collector surfaces was conducted. Figure 4 presents the calculated distribution of the tangential component of drag force that acts on bacterium in the vicinity of collectors from the three different porous media models, namely: single sphere (SS), two spheres in contact (TSIC), and two spheres not in contact (TSNIC). It should be noted that the presented distribution of the drag force is just for the top collector in the two spheres models. The magnitude of the tangential component of the drag force along the collector surface is plotted versus normalized distance (L/L_{max}), which is defined as the distance along the collector surface from the front to the rear stagnation point (L) divided by half the collector perimeter (L_{max}). As expected, the value of the drag force (and therefore $T_{driving}$) is dependent on the location along the collector surface. It is zero at the front and rear stagnation points (zero fluid velocity), and increases with the distance from these two points until it reaches a maximum value at the collector midpoint. Moreover, it is observed that values of the hydrodynamic drag force at locations near the rear stagnation point in the SS model are significantly higher than those associated with the TSIC and TSNIC models. The magnitude of drag force near the rear stagnation point also changes in a nonuniform fashion with L/L_{max} for the TSIC and TSNIC models. These observations will be explained further on in the manuscript.

[34] Figure 5 shows a plot of the fraction of surface area of the spherical collectors that may contribute to bacteria attachment (S_f) as a function of IS for the SS, TSIC, and TSNIC models. Assuming rolling is the principal mechanism for bacteria detachment, attachment occurs on the grain surface when $T_{resisting} > T_{driving}$. For all the models the value of S_f is unity when the IS reaches 100 mM, because attachment occurs in the primary minimum. The SS
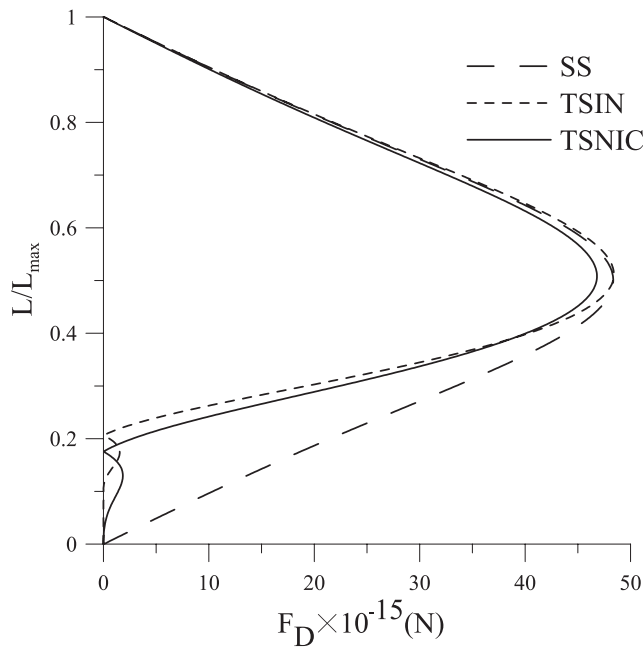
Figure 4. The calculated distribution of the tangential component of drag force that acts on a bacterial cell (assumed spherical shape) in the vicinity of the collectors for SS, TSIC, and TSNIC models of porous media. The average water velocity is 0.66 cm/min. The distribution of tangential drag force along the collector surface is plotted versus normalized distance (L/L_{max}), which is defined as the distance along the collector surface from the front to the rear stagnation point (L) divided by half the collector perimeter (L_{max}).

model predicts that the value of S_f is virtually zero for the lower three ionic strengths of 10, 30, and 50 mM (with a maximum of 0.1% for 50 mM), and implies that bacterial attachment will be negligible. Under these unfavorable attachment conditions ($T_{resisting} < T_{driving}$), bacteria that collided with the collector will be swept away by hydrodynamic shear. This result is in agreement with the results of batch experiments that indicated negligible attachment for ionic strengths less than or equal to 50 mM.

[35] In contrast to the SS model predictions, the values of S_f for the TSIC and TSNIC models are significantly higher for 10, 30, and 50 mM solutions and increases slowly with increasing IS. This observation suggests that lower drag forces occurred in some regions of the TSIC and TSNIC models as compared to the SS model. In fact, Figure 4 demonstrates that lower-velocity regions did occur near the rear stagnation point of the top sphere in the TSIC and TSNIC models. These regions may therefore contribute to greater bacteria retention even at low IS because $T_{resisting} > T_{driving}$ on these regions of the collectors.

[36] The torque balance calculations provide further explanation for the observed enhanced bacteria retention in the column experiments as compared to the batch studies. However, the torque balance calculations shown in Figure 5 indicates that S_f will increase very slowly with increasing IS when the IS was less than or equal to 50 mM. In contrast, Figure 2 indicates that colloid retention behavior was a strong function of solution IS over this same IS range.

Moreover, the torque balance calculations predict that the value of S_f is negligible for all three models when the IS of 1 mM was considered in these calculations (data not shown). This implies that if the resisting and driving torques (hydrodynamic and physicochemical forces) were the main mechanism for bacteria retention, the retained bacteria should have been released upon introduction of low-solution IS. In contrast, the elution experiments shown in Figure 3 indicate that only a fraction of the retained bacteria were released after flushing the column with 1 mM solution. This apparent discrepancy suggests that the underlying mechanisms for bacterial retention are interconnected and likely depends on other factors not considered in this analysis.

3.5. Immobile Zones and Cell Retention

[37] Additional flow simulations were conducted to examine the fluid flow field near the rear stagnation point of the SS, TSIC, and TSNIC models. Figure 6a shows the streamlines and normalized velocity arrows in regions near the rear stagnation point for these models under conditions of steady flow at a low Reynolds number. As expected, flow in the SS model follow the collector surface and no separation of the fluid streamlines from the collector surface is observed (Figure 6). In contrast, the pore space geometry of the TSIC and TSNIC models causes fluid streamlines to separate from the collector surface, and to form immobile regions near the gap between the two grains. In these immobile regions, where water does not mix with the bulk solution, water rotates in an infinite set of nested ring vortices (Figures 6b and 6c). This type of behavior of Stokes flow around two spheres in contact or close to each other has theoretically been demonstrated [e.g., *Davis et al.*, 1976; *Davis and O'Neill*, 1977] and experimentally visualized by *Taneda* [1979]. Indeed, the unusual behavior of the tangential component of the drag force shown in Figure 4
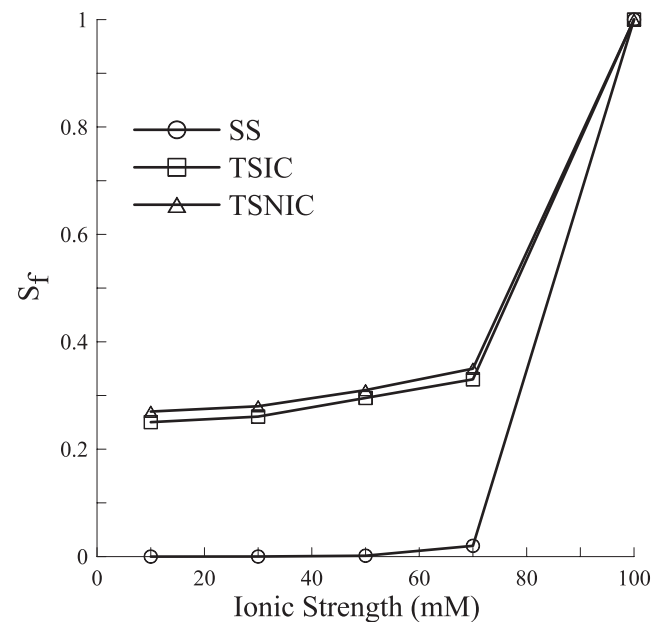

Figure 5. Plot of the fraction of the surface area of the collectors that may contribute to bacteria attachment (S_f) as a function of ionic strength for three different models (SS, TSIC, and TSNIC) in the presence of an average pore water velocity of 0.66 cm/min.
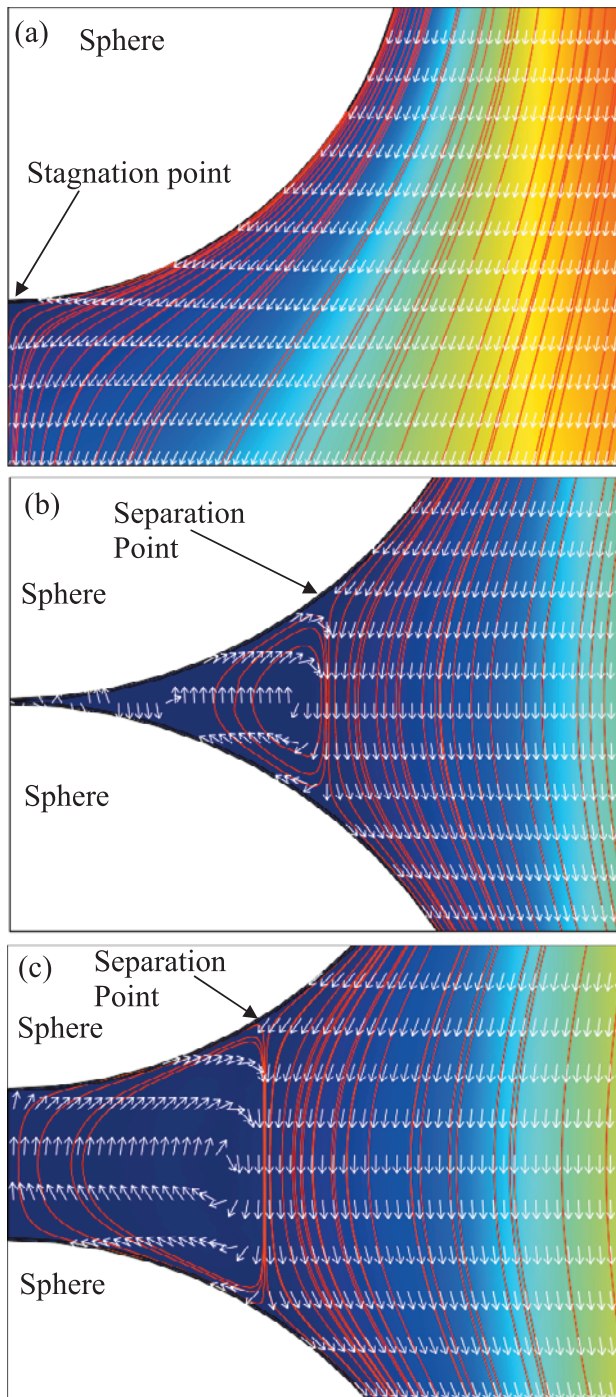
Figure 6. The simulated velocity field near the rear stagnation point of (a) the SS model and near the gap between the two spheres in (b) TSIC and (c) TSNIC models. In the case of TSIC and TSNIC models, separation of streamlines (red lines) from the collector surface occurs and produces an immobile region within the gap between the two spheres. The white arrows are the normalized water velocity indicating that water rotates with a very low velocity in the immobile regions.

for the TSIC and TSNIC models can be explained by the existence of a complex flow field (nested ring vortices) in the gap region between the two spheres. It should be mentioned that immobile regions in porous media, espe-

cially unsaturated conditions, have been used to explain a variety of observed transport behavior without recognizing the exact system hydrodynamics [*Toride et al.*, 2003; *Padilla et al.*, 1999].

[38] The insight obtained from studying the flow structure near the contact point in TSIC model and around the gap between two spheres in the TSNIC model may clarify the mechanism of bacteria or in general colloid retention in porous media. When the porous media is static (e.g., column experiments), the pore space geometry will produce many hydrodynamically disconnected (immobile) regions (Figures 6b and 6c). Once the colloids or bacterial cells enter these regions, they will be retained, even under unfavorable attachment conditions. The only way that colloids may escape these immobile zones is through Brownian diffusion. This important finding provides one reasonable explanation for the observations that a small fraction of the retained bacteria were released after flushing the columns with low IS solution (Table 2). It also provides an explanation for differences in bacteria retention in batch and column experiments. During batch experiments the porous media is in constant motion which does not allow immobile regions to exist. Under these conditions, bacteria retention may only occur when the resisting torque (physicochemical forces) is greater than the driving torque (hydrodynamic forces); i.e., the 100 mM batch experiment.

[39] It should be mentioned that the magnitude of the fluid velocity in the immobile zones (hydrodynamically disconnected regions) is very small. This results in small drag forces in these regions, and the bacteria cells therefore have a greater chance to attach to the collector surface (Figure 5). Even if the conditions are not favorable for bacteria attachment to the solid surface in these immobile regions (e.g., $T_{resisting} < T_{driving}$), the cells will still continue to circulate within these zones and will therefore be released back into the bulk solution primarily by diffusion. It is also likely that bacteria-bacteria interactions will be enhanced in immobile zones because the number of bacteria collisions may drastically increase relative to that in bulk solution. As bacteria accumulation continues and starts to fill the immobile zones, the pore space geometry will become a limiting factor in bacteria retention. Indeed, fluorescent microscopy and x-ray microtomography studies have demonstrated that colloids accumulate in the narrow region of the pore spaces near the contacts of irregularly shaped sand grains under unfavorable attachment conditions [*Bradford et al.*, 2005, 2006; *Xu et al.*, 2006; *Li et al.*, 2006; *Yoon et al.*, 2006]. In these studies, pore-space constrictions apparently served as locations for colloid retention, whereas few colloids appeared to be immobilized far from the grain-to-grain contacts. Colloid retention in the smallest regions of the pore space such as those formed near grain to grain contact points has been referred to in the literature as straining [*Hill*, 1957; *McDowell-Boyer et al.*, 1986; *Cushing and Lawler*, 1998; *Bradford et al.*, 2006].

3.6. Coupling of Factors in Cell Retention

[40] Colloid retention behavior was found to be a strong function of solution IS under unfavorable conditions. This dependency can be explained by considering mechanisms of bacteria transfer to hydrodynamically disconnected immobile regions. According to conventional filtration theory, bacteria may collide with grain surfaces via sedimentation,

interception, and diffusion [*Yao et al.*, 1971]. Bacteria cells that are weakly associated with the solid-water interface via the secondary energy minimum, however, experience significant hydrodynamic forces owing to fluid flow that may result in bacteria detachment via rolling or sliding [*Tsai et al.*, 1991; *Bergendahl and Grasso*, 1998, 1999; *Torkzaban et al.*, 2007]. Some of these weakly associated bacteria can be translated and/or funneled by fluid drag forces to immobile regions (e.g., grain-to-grain contact points) and be retained in these straining sites [*Bradford et al.*, 2007]. Increasing the IS results in a greater depth of secondary energy minimum (see Table 2) which likely leads to larger numbers of bacteria (rolling or sliding along the solid surface) and entering the immobile zones. Indeed, recent experimental evidence by *Kuznar and Elimelech* [2007] demonstrates that colloids captured in the secondary energy minimum can be translated along the collector surface via hydrodynamic forces and be retained in regions near the rear stagnation point. Once again, these findings provide a plausible explanation for the observed dependence of bacteria retention on solution IS shown and in particular, the coupled effect of solution chemistry, pore structure, and system hydrodynamics on bacteria retention.

[41] It should be mentioned that straining has traditionally been assumed to be purely a physical phenomena [*Herzig et al.*, 1970; *McDowell-Boyer et al.*, 1986] and therefore only determined by geometry considerations. Recent experimental evidence, however, indicates a strong coupling of straining on solution chemistry and hydrodynamics [*Bradford et al.*, 2006, 2007; *Torkzaban et al.*, 2008]. This work provides additional experimental and theoretical understanding of the coupling of chemical conditions and pore space geometry on straining. In particular, the role of pore-scale hydrodynamics on colloid retention is clarified.

4. Summary and Conclusions

[42] Experimental evidence in this study has demonstrated that solution chemistry and bacteria attachment are not the only factors and mechanisms responsible for bacteria retention. In particular, the data indicates that pore space geometry also played an important role in bacteria retention. The first piece of indirect evidence are results from batch experiments (where the pore structure was eliminated) which found no significant bacterial attachment to the sand when the IS was less than or equal to 50 mM. Second, reducing the IS in column experiments to a very low value (1 mM) only resulted in release of a fraction of the retained bacteria that were deposited under higher IS conditions. Finally, column mass balance indicates that good recovery of the retained bacteria was achieved when the pore structure was destroyed by suspending the sand in excess amounts of solution of the same IS that was used in the transport experiments. Computer simulation results also confirm the importance of the system hydrodynamics. The pore space geometry formed near grain to grain contact points was found to produce hydrodynamically disconnected regions. These immobile zones contain an infinite set of nested ring vortices that can significantly contribution to bacteria retention. It is possible that these hydrodynamically disconnected regions may also occur in other locations in porous media; e.g., near rough surfaces on collectors and adjacent to dead end regions of the pore space.

These computer simulations provide an explanation for differences in retention behavior in batch and column experiments, as well as the incomplete recovery of retained colloids when the columns were flushed with a low IS solution.

[43] The observed increasing amount of bacteria retention with increasing IS was explained by considering the mass transfer of bacteria (rolling along the interface) to the immobile regions of the pore medium. In particular, increasing the IS results in a greater depth of the secondary energy minimum (see Table 2) which likely leads to greater numbers of bacteria being transported along the solid surface by hydrodynamic forces to these regions (straining locations). Hence, bacteria retention in porous media is a coupled process that strongly depends on solution chemistry, pore structure, and system hydrodynamics.

References

Ahmadi, G., S. Guo, and X. Zhang (2007), Particle adhesion and detachment in turbulent flows including capillary forces, *J. Particulate Sci. Technol.*, *25*, 59–76.

Azeredo, J., I. Visser, and R. Oliveira (1999), Exopolymers in bacterial adhesion: Interpretation in terms of DLVO and XDLVO theories, *Colloids Surf B*, *14*, 141–148.

Bergendahl, J., and D. Grasso (1998), Colloid generation during batch leaching tests: Mechanics of disaggregation, *Colloids Surf A*, *135*, 193–205.

Bergendahl, J., and D. Grasso (1999), Prediction of colloid detachment in a model porous media: Thermodynamics, *AIChE J.*, *45*(3), 475–484.

Bergendahl, J., and D. Grasso (2000), Prediction of colloid detachment in a model porous media: Hydrodynamics, *Chem. Eng. Sci.*, *55*, 1523–1532.

Bird, R. B., W. E. Stewart, and E. N. Lightfoot (2002), *Transport Phenomena*, 2nd ed., John Wiley, Hoboken, N. J.

Bradford, S. A., S. R. Yates, M. Bettahar, and J. Simunek (2002), Physical factors affecting the transport and fate of colloids in saturated porous media, *Water Resour Res.*, *38*, 1327–1338.

Bradford, S. A., J. Simunek, M. Bettahar, Y. F. Tadassa, M. T. van Genuchten, and S. R. Yates (2005), Straining of colloids at textural interfaces, *Water Resour. Res.*, *41*, W10404, doi:10.1029/2004WR003675.

Bradford, S. A., J. Simunek, M. Bettahar, M. T. van Genuchten, and S. R. Yates (2006), Significance of straining in colloid deposition: Evidence and implications, *Water Resour. Res.*, *42*, W12S15, doi:10.1029/2005WR004791.

Bradford, S. A., S. Torkzaban, and S. L. Walker (2007), Coupling of physical and chemical mechanisms of colloid straining in saturated porous media, *Water Res.*, *41*, 3012–3024.

Camesano, T. A., and B. E. Logan (1998), Influence of fluid velocity and cell concentration on the transport of motile and non-motile bacteria in porous media, *Environ. Sci. Technol.*, *32*, 1699–1708.

Cooley, M. D. A., and M. E. O'Neill (1969), On the slow motion of two spheres in contact along their line of centers in a viscous fluid, *Proc. Cambridge Philos. Soc.*, *66*, 407.

Cushing, R. S., and D. F. Lawler (1998), Depth filtration: Fundamental investigation through three-dimensional trajectory analysis, *Environ. Sci. Technol.*, *32*, 3793–3801.

Davis, A. M. J., and M. E. O'Neill (1977), Separation in a slow linear shear flow past a cylinder and a plane, *J. Fluid Mech.*, *81*, 551–564.

Davis, A. M. J., M. E. O'Neill, J. M. Dorrepaal, and K. B. Ranger (1976), Separation from the surface of two equal spheres in Stokes flow, *J. Fluid Mech.*, *77*, 625–644.

Derjaguin, B. V., and L. Landau (1941), Theory of stability of strongly charged lyophobic sols and of the adhesion of strongly charged particles in solutions of electrolytes, *Acta Physicochim. URSS*, *14*, 633–662.

Elimelech, M., J. Gregory, X. Jia, and R. A. Williams (1998), *Particle Deposition and Aggregation Measurement, Modeling and Simulation*, Elsevier, New York.

Foppen, J. W. A., and J. F. Schijven (2006), Evaluation of data from the literature on the transport and survival of Escherichia coli and thermotolerant coliforms in aquifers under saturated conditions, *Water Res.*, *40*, 401–426.

Franchi, A., and C. R. O'Melia (2003), Effects of natural organic matter and solution chemistry on the deposition and reentrainment of colloids in porous media, *Environ. Sci. Technol.*, *37*, 1122–1129.

Gannon, J. T., V. B. Manilal, and M. Alexander (1991), Relationship between cell surface properties and transport of bacteria through soil, *Appl. Environ. Microbiol.*, *57*, 190–193.

Ginn, T. R., B. D. Wood, K. E. Nelson, T. D. Scheibe, E. M. Murphy, and T. P. Clement (2002), Processes in microbial transport in the natural subsurface, *Adv. Water Res.*, *25*, 1017–1042.

Goldman, A. J., R. G. Cox, and H. Brenner (1967), Slow viscous motion of a sphere parallel to a plane wall: Couette flow, *Chem. Eng. Sci.*, *22*, 653–660.

Gregory, J. (1981), Approximate expression for retarded van der Waals interaction, *J. Colloid Interface Sci.*, *83*, 138–145.

Gross, M., S. E. Cramton, F. Gotz, and A. Peschel (2001), Key role of Teichoic acid net charge in Staphylococcus aureus colonization of artificial surfaces, *Infect. Immun.*, *69*, 3423–3426.

Hahn, M. W., and C. R. O'Melia (2004), Deposition and reentrainment of Brownian particles in porous media under unfavorable chemical conditions: Some concepts and applications, *Environ. Sci. Technol.*, *38*, 210–220.

Hahn, M. W., D. Abadzic, and C. R. O'Melia (2004), Aquasols: On the role of secondary minima, *Environ. Sci. Technol.*, *38*, 5915–5924.

Happel, J. (1958), Viscous flow in multiparticle systems: Slow motion of fluids relative to beds of spherical particles, *AIChE J.*, *4*, 197–201.

Harvey, R. W., and H. Harms (2001), Transport of microorganisms in the terrestrial subsurface: In situ and laboratory methods, in *Manual of Environmental Microbiology*, 2nd ed., edited by C. J. Hurst et al., chap. 69, pp. 753–776, Am. Sci. for Microbiol. Press, Washington, D. C.

Herald, P. J., and E. A. Zottola (1989), Effect of various agents upon the attachment of Pseudomonas fragi to stainless steel, *J. Food Sci.*, *54*, 461–464.

Herzig, J. P., D. M. Leclerc, and P. LeGoff (1970), Flow of suspension through porous media: Application to deep filtration, *Ind. Eng. Chem. Res.*, *62*, 129–157.

Hill, W. A. (1957), An analysis of sand filtration, *J. Sanitary Eng. Div.*, *83*, 12,761–12,769.

Hogg, R., T. W. Healy, and D. W. Fuerstenau (1966), Mutual coagulation of colloidal dispersions, *Trans. Faraday Soc.*, *62*, 1638–1651.

Israelachvili, J. N. (1992), *Intermolecular and Surface Forces*, 2nd ed., Academic, Elsevier, New York.

Jewett, D. G., T. A. Hilbert, B. E. Logan, R. G. Arnold, and R. C. Bales (1995), Bacterial transport in two porous media systems: Influence of ionic strength and pH on collision efficiency, *Water. Res.*, *29*, 1673–1680.

Johnson, K. L. (1985), *Contact Mechanics*, Cambridge Univ. Press, New York.

Johnson, K. L., K. Kendall, and A. D. Roberts (1971), Surface energy and the contact of elastic solids, *Proc. R. Soc. London*, *324*, 301–313.

Kuznar, Z. A., and M. Elimelech (2007), Direct microscopic observation of particle deposition in porous media: Role of the secondary energy minimum, *Colloids Surf. A*, *294*, 156–162.

Li, X., T. D. Scheibe, and W. P. Johnson (2004), Apparent decreases in colloid deposition rate coefficient with distance of transport under unfavorable deposition conditions: A general phenomenon, *Environ. Sci. Technol.*, *38*, 5616–5625.

Li, X., C. Lin, J. D. Miller, and W. P. Johnson (2006), Pore-scale observation of microsphere deposition at grain-to-grain contacts over assemblage-scale porous media domains using X-ray microtomography, *Environ. Sci. Technol.*, *40*, 3762–3768.

Marquardt, D. W. (1963), An algorithm for least squares estimation of nonlinear parameters, *SIAM. J. Appl. Math.*, *11*, 431–441.

Martin, R. E., L. M. Hanna, and E. J. Bouwer (1991), Determination of bacterial collision efficiencies in a rotating disk system, *Environ. Sci. Technol.*, *25*, 2075–2082.

McDowell-Boyer, L. M., J. R. Hunt, and N. Sitar (1986), Particle transport through porous media, *Water Resour. Res.*, *22*, 1901–1921.

Meinders, J. M., H. C. van der Mei, and H. J. Busscher (1995), Deposition efficiency and reversibility of bacterial adhesion under flow, *J. Colloid Interface Sci.*, *176*, 329–341.

Murphy, E. M., and T. R. Ginn (2000), Modeling microbial processes in porous media, *Hydrogeol. J.*, *8*, 142–158.

O'Neill, M. E. (1968), A sphere in contact with a plane wall in a slow linear shear flow, *Chem. Eng. Sci.*, *23*, 1293–1298.

Padilla, I. Y., T. C. Jim Yeh, and M. H. Conklin (1999), The effect of water content on solute transport in unsaturated porous media, *Water Resour. Res.*, *35*, 3303–3313.

Payatakes, A. C., R. Rajagopalan, and C. Tien (1974), On the use of Happel's Model for filtration studies, *J. Colloid Interface Sci.*, *49*, 321.

Poortinga, A. T., R. Bos, W. Norde, and H. J. Busscher (2002), Electric double layer interactions in bacterial adhesion to surfaces, *Surf. Sci.*, *47*, 1–32.

Redman, J. A., S. L. Walker, and M. Elimelech (2004), Bacterial adhesion and transport in porous media: Role of the secondary energy minimum, *Environ. Sci. Technol.*, *38*, 1777–1785.

Rijnaarts, H. H. M., W. Norde, E. J. Bouwer, J. Lyklema, and A. J. B. Zehnder (1995), Reversibility and mechanism of bacterial adhesion, *Colloids Surf. B*, *4*, 5–22.

Ryan, J. N., and M. Elimelech (1996), Colloid mobilization and transport in groundwater, *Colloids Surf. A*, *107*, 1–56.

Schafer, A., H. Harms, and A. J. B. Zehnder (1998), Bacterial accumulation at the air-water interface, *Environ. Sci. Technol.*, *32*, 3704–3712.

Sharma, M. M., H. Chamoun, D. S. H. Sita Rama Sarma, and R. S. Schechter (1992), Factors controlling the hydrodynamic detachment of particles from surfaces, *J. Colloid Interface Sci.*, *149*, 121–134.

Simoni, S. F., T. N. P. Bosma, H. Harms, and A. J. B. Zehnder (2000), Bivalent cations increase both the subpopulation of adhering bacteria and their adhesion efficiency in sand columns, *Environ. Sci. Technol.*, *34*, 1011–1017.

Simunek, J., M. T. van Genuchten, and M. Sejna (2005), *The HYDRUS-1D Software Package for Simulating the One-Dimensional Movement of Water, Heat, and Multiple Solutes in Variably-Saturated Media—Version 3.0, HYDRUS Software Ser.*, vol. 1, 240 pp., Dep. of Environ. Sci., Univ. of Calif., Riverside, Calif.

Smets, B. F., D. Grasso, M. A. Engwall, and B. J. Machinist (1999), Surface physicochemical properties of Pseudomonas fluorescens and impact on adhesion and transport through porous media, *Colloids Surf. B*, *14*, 121–139.

Soltani, M., and G. Ahmadi (1994), On particle adhesion and removal mechanisms in turbulent flows, *J. Adhesion Sci. Technol.*, *7*, 763–785.

Stimson, M., and G. B. Jeffery (1926), The motion of two spheres in a viscous fluid, *Proc. R. Soc. London A*, *111*, 110.

Taneda, S. (1979), Visualization of separating Stokes flows, *J. Phys. Soc. Jpn.*, *46*, 1935–1942.

Toride, N., M. Inoue, and F. J. Leij (2003), Hydrodynamic dispersion in an unsaturated dune sand, *Soil Sci. Soc. Am. J.*, *67*, 703–712.

Torkzaban, S., S. A. Bradford, and S. L. Walker (2007), Resolving the coupled effects of hydrodynamics and DLVO forces on colloid attachment in porous media, *Langmuir*, *23*(19), 9652–9660, doi:10.1021/la700995e.

Torkzaban, S., S. A. Bradford, M. T. van Genuchten, and S. L. Walker (2008), Colloid transport in unsaturated porous media: The role of water content and ionic strength on particle straining, *J. Contam. Hydrol.*, *96*, 113–128.

Truesdail, S. E., J. Lukasik, S. R. Farrah, D. O. Shah, and R. B. Dickinson (1998), Analysis of bacterial deposition on metal (hydr)oxide-coated sand filter media, *J. Colloid Interface Sci.*, *203*, 369–378.

Tsai, C. J., D. Y. H. Pui, and B. Y. H. Liu (1991), Particle detachment from disk surfaces of computer disk drives, *J. Aerosol Sci.*, *22*, 737–746.

Tufenkji, N., and M. Elimelech (2004), Deviation from the classical colloid filtration theory in the presence of repulsive DLVO interactions, *Langmuir*, *20*, 10,818–10,828.

Tufenkji, N., and M. Elimelech (2005), Breakdown of colloid filtration theory: Role of the secondary energy minimum and surface charge heterogeneities, *Langmuir*, *21*, 841–852.

van Loosdrecht, M. C. M., J. Lyklema, W. Norde, G. Schraa, and A. J. B. Zehnder (1987a), Electrophoretic mobility and hydrophobicity as a measure to predict the initial steps of bacterial adhesion, *Appl. Environ. Microbiol.*, *53*, 1898–1901.

van Loosdrecht, M. C. M., J. Lyklema, W. Norde, G. Schraa, and A. J. B. Zehnder (1987b), The role of bacterial cell wall hydrophobicity in adhesion, *Appl. Environ. Microbiol.*, *53*, 1893–1897.

Verwey, E. J. W., and J. T. G. Overbeek (1948), *Theory of the Stability of Lyophobic Colloids*, Elsevier, New York.

Vigeant, M. A. S., R. M. Ford, M. Wagner, and L. K. Tamm (2002), Reversible and irreversible adhesion of motile Escherichia coli cells analyzed by total internal reflection aqueous fluorescence microscopy, *Appl. Environ. Microbiol.*, *68*, 2794–2801.

Walker, S. L., J. A. Redman, and M. Elimelech (2004), Role of cell surface lipopolysaccharides in Escherichia coli K12 adhesion and transport, *Langmuir*, *20*, 7736–7746.

Xu, S., B. Gao, and J. E. Saiers (2006), Straining of colloidal particles in saturated porous media, *Water Resour. Res.*, *42*, W12S16, doi:10.1029/2006WR004948.

Yao, K. M., M. T. Habibian, and C. R. Omelia (1971), Water and waste water filtration concepts and applications, *Environ. Sci. Technol.*, *l5*, 1105–1112.

Yoon, J. S., J. T. Germaine, and P. J. Culligan (2006), Visualization of particle behavior within a porous medium: Mechanisms for particle filtration and retardation during downward transport, *Water Resour. Res.*, *42*, W06417, doi:10.1029/2004WR003660.

———————————————

S. A. Bradford, U.S. Salinity Laboratory, Agricultural Research Service, U.S. Department of Agriculture, 450 W. Big Springs Road, Riverside, CA 92507-4617, USA. (sbradford@ussl.ars.usda.gov)

S. S. Tazehkand, Department of Earth Sciences, Utrecht University, P.O. Box 80021, NL-3508TA Utrecht, Netherlands.

S. Torkzaban and S. L. Walker, Department of Chemical and Environmental Engineering, University of California, Riverside, CA 92521, USA.